

Modular TM_1 mixing in light of precision measurement in JUNO

Wen-Hao Jiang,^{1 a,b,c} Ruiwen Ouyang,^{2 a} and Ye-Ling Zhou^{3 a}

^a School of Fundamental Physics and Mathematical Sciences,
Hangzhou Institute for Advanced Study, UCAS, Hangzhou 310024, China

^b Institute of Theoretical Physics, Chinese Academy of Sciences, Beijing 100190, China

^c University of Chinese Academy of Sciences, Beijing 100049, China

Abstract

This paper investigates the landscape of models based on modular S_4 symmetry that predicts the trimaximal TM_1 mixing pattern for leptonic flavor mixing, and explores their parameter spaces with constraints from the latest high-precision measurement on θ_{12} and Δm_{21}^2 given by JUNO experiment. We review on how the mixing pattern arises from residual symmetries after the spontaneous breaking of a flavor symmetry, via an appropriate vacuum alignment of modular fields and flavon fields. We show three different models that realize the TM_1 in three approaches with the same symmetry structure. Due to different model building strategies used, predictions on the CP-violating phase and the effective mass in neutrinoless double beta decay are different, making them distinguishable.

¹jiangwenhao25@mails.ucas.ac.cn

²ruiwen.ouyang@ucas.ac.cn

³zhouyeling@ucas.ac.cn

1 Introduction

Leptonic flavor mixing remains a mystery in particle physics. Following decades of sustained and systematic efforts, three mixing angles and two mass-squared differences have been measured [1]. The coming goals are the determination of neutrino mass ordering (normal $m_1 < m_2 < m_3$ or inverted $m_3 < m_1 < m_2$) and measurement of the Dirac phase δ . JUNO [2], Hyper-K [3] and DUNE [4], the three representative large-scale neutrino oscillation experiments of this stage, aim to achieve these goals. In the meantime, measurements of other oscillation parameters with precision at sub-percent level will be performed. After less than two months of running, JUNO released the first data on the measurement of Δm_{21}^2 and $\sin^2 \theta_{12}$ with best-fit values $\pm 1\sigma$ given by [5]

$$\Delta m_{21}^2 = (7.50 \pm 0.12) \times 10^{-5} \text{ eV}^2, \quad \sin^2 \theta_{12} = 0.3092 \pm 0.0087, \quad (1)$$

for the normal mass ordering scenario, which already showed a better precision than the previous global fit for all past measurements [6].

To explain the observed neutrino oscillation parameters, various of simple mixing ansatzes for the lepton flavor mixing were proposed. Due to their simplicity in describing experimental data and predictability from flavor symmetries, they have been widely studied in neutrino theories (see, e.g., reviews [7–10]). Of particular example is a constant mixing pattern called tri-bimaximal (TBM) mixing [11, 12], although it has been excluded by the observation of a relatively large θ_{13} in reactor neutrino experiments [13, 14]. Among series of pre-existing simple mixing patterns in the literature, the trimaximal TM_1 mixing [15, 16, 18–20], a partially constant mixing which inherits the first column the TBM form, offers an elegant description for the observed lepton mixing.

For better understanding the trimaximal TM_1 mixing pattern, non-Abelian discrete symmetries were introduced as origins of flavor mixing, and a particular mixing pattern arises from the spontaneous breaking of the flavor symmetry. For example, the TBM pattern can be realized from the permutation group S_4 . It is enforced if the charged lepton mass term keep a Z_3^T symmetry and the neutrino mass term is invariant under Z_2^S and Z_2^U symmetries, all of which are residual symmetries after S_4 breaking [21]⁴. Relaxing the residual symmetry in the neutrino sector to be Z_2^{SU} gives rise to TM_1 mixing [22, 23]. In the traditional flavor symmetry approach, the symmetry breaking is achieved via vacuum expectation values (VEVs) of a series of scalar fields which are called flavons, and the flavor texture succeeds the special direction of the VEV alignment.

Modular symmetries, as a non-linearly realized approach, provide an alternative explanation that the flavor texture might arise from modular forms of a modular symmetry [24]. Here a modular form is a holomorphic function of the modular field τ and the symmetry breaking as well as the special pattern of modular forms are achieved via the VEV of the modular field. In the minimal setup (e.g. [25, 26]) it only needs a modular field, which has only two real degrees of freedom, acquiring a VEV, without the necessity of introducing many flavon fields aligned in some specific ways (e.g. [17]), to achieve the desired phenomenology. Thus, this approach reduces physical degrees of freedom very efficiently.

A modulus field may gain the VEV at a fixed point, which is invariant under certain modular transformations. The lepton mass matrix at the fixed point preserves a residual symmetry as a subgroup of the modular symmetry. Implications of residual modular

⁴ T , S and U are generators of S_4 satisfying $T^3 = S^2 = U^2 = (SU)^2 = (TU)^2 = (ST)^3 = (STU)^4 = 1$.

symmetries were suggested in the derivation of simple structures of modular forms [26]. However, the minimal setup is not enough to accommodate the observed lepton mixing because a single modular field cannot achieve the misalignment of different residual symmetries in the charged lepton sector and neutrino sector [27]. Necessary extensions must be considered in realistic models. For example, by introducing a minimal set of flavons in the modular symmetry, the modular symmetry is broken differently for charged leptons and neutrinos via the flavon and modular field, respectively [28]. Another approach is including distinguishable modulus fields in the framework of multiple modular symmetries [29]. This approach allows different residual symmetries from fixed points, e.g., $\tau_l = -\frac{1}{2} + i\frac{\sqrt{3}}{2}$ respecting Z_3^T and $\tau_\nu = -\frac{1}{2} + \frac{i}{2}$ respecting Z_2^{SU} , predicting exactly TM₁ mixing [30].

The present paper aims to investigate the landscape of modular S_4 models that realize the TM₁ mixing and explore their parameter spaces with constraints from the latest precision measurements in JUNO. We sketch three possible approaches with modular symmetries in Fig. 1. The rest of the paper is organized as follows. We begin with a review of the trimaximal TM₁ mixing pattern in Section 2. We revisit the mathematical correlation between TM₁ and residual symmetries Z_3^T , Z_2^{SU} of S_4 , regardless of the traditional flavor symmetry approach or modular symmetry approach. This implies that one can take approaches in Figure 1 to build concrete models featuring the TM₁ mixing. In Section 3, we present explicit models with modular S_4 flavor symmetry, which feature TM₁ but give different predictions on other observables. We perform numerical scans to fit these models in Section 4. The summary and conclusions are presented in Section 5.

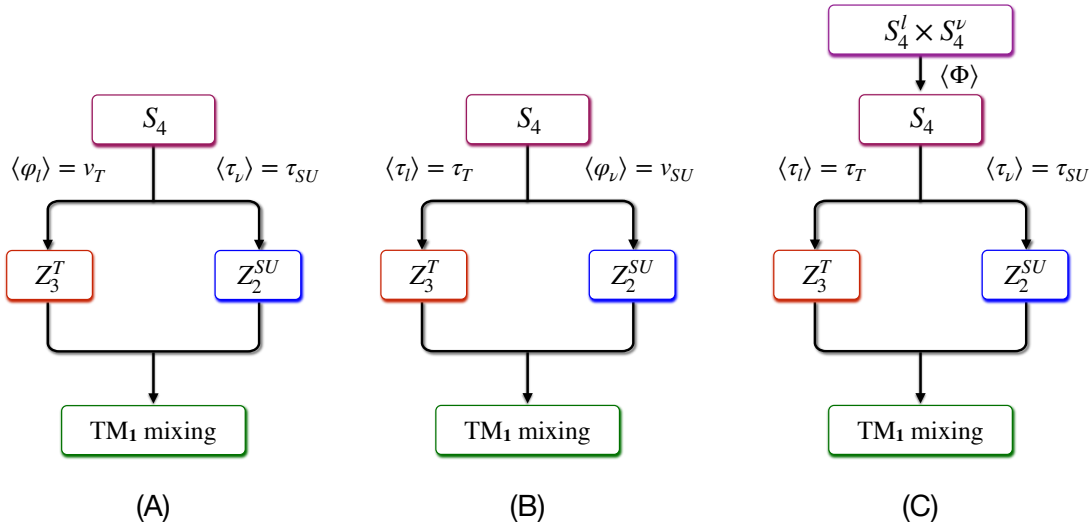


Figure 1: A few approaches to realise TM₁ mixing in modular flavour models.

2 Trimaximal TM_1 mixing

2.1 TM_1 mixing in light of recent data

We begin by reviewing the trimaximal mixing used to explain the neutrino mixings in the literature. The PMNS matrix can be parameterized as [1]:

$$U_{\text{PMNS}} = \begin{pmatrix} c_{12}c_{13} & s_{12}c_{13} & s_{13}e^{-i\delta} \\ -s_{12}c_{23} - c_{12}s_{13}s_{23}e^{i\delta} & c_{12}c_{23} - s_{12}s_{13}s_{23}e^{i\delta} & c_{13}s_{23} \\ s_{12}s_{23} - c_{12}s_{13}c_{23}e^{i\delta} & -c_{12}s_{23} - s_{12}s_{13}c_{23}e^{i\delta} & c_{13}c_{23} \end{pmatrix} \begin{pmatrix} 1 & 0 & 0 \\ 0 & e^{i\frac{\alpha_{21}}{2}} & 0 \\ 0 & 0 & e^{i\frac{\alpha_{31}}{2}} \end{pmatrix}, \quad (2)$$

where $s_{ij} = \sin \theta_{ij}$, $c_{ij} = \cos \theta_{ij}$ for three mixing angles θ_{12} , θ_{13} , θ_{23} , δ is the Dirac phase, and α_{21} , α_{31} are irremovable Majorana phases for Majorana neutrinos. A particular mixing pattern, giving $s_{12}^2 = 1/3$, $s_{13}^2 = 0$, and $s_{23}^2 = 1/2$, is the so-called tri-bimaximal (TBM) mixing pattern [11, 12], with each entry, up to a phase difference, being constant,

$$U_{\text{TBM}} = \begin{pmatrix} \frac{2}{\sqrt{6}} & \frac{1}{\sqrt{3}} & 0 \\ \frac{-1}{\sqrt{6}} & \frac{1}{\sqrt{3}} & \frac{1}{\sqrt{2}} \\ \frac{-1}{\sqrt{6}} & \frac{1}{\sqrt{3}} & \frac{-1}{\sqrt{2}} \end{pmatrix}. \quad (3)$$

This mixing ansatz is apparently excluded due to the nonzero mixing angle θ_{13} , but still well approximates the observed values of θ_{12} and θ_{23} in the 3σ regimes. An extension of the TBM ansatz was thus proposed to incorporate the small but not tiny reactor angle θ_{13} [16], where the lepton mixing matrices still preserve the first column of the TBM ansatz and leave the rest parameters unfilled, which is now called the trimaximal mixing ansatz, TM_1 ,

$$U_{\text{TM}_1} = \begin{pmatrix} \frac{2}{\sqrt{6}} & \times & \times \\ \frac{-1}{\sqrt{6}} & \times & \times \\ \frac{-1}{\sqrt{6}} & \times & \times \end{pmatrix} \quad (4)$$

up to phase differences, where the unfilled parameters can be fixed once the reactor angle θ_{13} is specified. The TM_1 mixing leaves two sum rules between mixing angles and the CP phase,

$$\begin{aligned} \text{TM}_1 : \quad \sin^2 \theta_{12} &= 1 - \frac{2}{3(1 - \sin^2 \theta_{13})}, \\ \theta_{23} &\approx 45^\circ + \sqrt{2}\theta_{13} \cos \delta, \end{aligned} \quad (5)$$

The first sum in the above equation is enforced by the constant absolute value $|(U_{\text{TM}_1})_{e1}| = 2/\sqrt{6}$, and the second sum rule is derived perturbatively for small θ_{13} after a 2-3 unitary matrix taken into account [17]. Another widely studied mixing pattern is the TM_2 mixing, which preserves the second column of TBM,

$$U_{\text{TM}_2} = \begin{pmatrix} \times & \frac{1}{\sqrt{3}} & \times \\ \times & \frac{1}{\sqrt{3}} & \times \\ \times & \frac{1}{\sqrt{3}} & \times \end{pmatrix}, \quad (6)$$

up to phase differences, and predicts sum rule between mixing angles and CP phase [17]

$$\text{TM}_2 : \quad \sin^2 \theta_{12} = \frac{1}{3(1 - \sin^2 \theta_{13})},$$

$$\theta_{23} \approx 45^\circ + \frac{1}{\sqrt{2}} \theta_{13} \cos \delta. \quad (7)$$

Correlations between θ_{12} and θ_{13} in both TM_1 and TM_2 are presented in Fig. 2. Given the values of θ_{13} from reactor experiments, the trimaximal TM_2 mixing ansatz predicts $\theta_{12} \approx 36^\circ$, which is not consistent with JUNO data in 3σ region, as seen in the figure, even including the renormalization group (RG) effect running from a very high energy scale of the Standard Model [32]. On the other hand, TM_1 predicts $\theta_{12} \approx 34^\circ$ for $\theta_{13} \approx 8.5^\circ$. This is marginally touch to 1σ boundary of JUNO data, where $\sin^2 \theta_{12} = 0.309 \pm 0.009$ [5], as shown in the Figure 2. It can fit the JUNO data better if the small RG running effect is included [32]. Therefore, in the following sections, we will mainly focus on the TM_1 mixing. For the sum rule between θ_{23} and the CP phase δ in light of the recent data, we refer to reference [31].

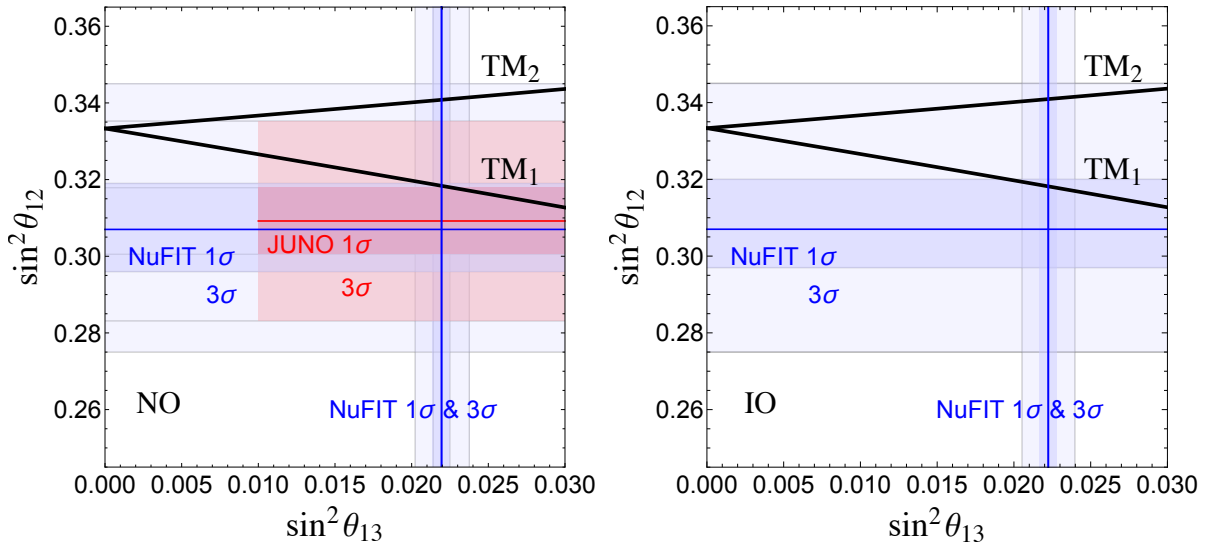


Figure 2: Sum rules between θ_{12} and θ_{13} in TM_1 and TM_2 mixing. best-fits, 1σ and 3σ ranges from NuFIT 6.0 (green) [6] and the first run of JUNO (red) [5] are shown as comparison.

2.2 TM_1 mixing predicted in flavor symmetries

Three different approaches presented in Fig. 1 show the connection between those discrete residual symmetries and the mixing pattern of the PMNS matrix. In this section, we show a general symmetry-based deduction that the same mixing pattern can be achieved regardless of the different approaches taken. Before turn to realistic models, we give a brief review on how leptonic mixing arise from residual symmetries of a flavor symmetry and in particular TM_1 mixing from residual symmetries of S_4 .

Let us start by considering the complete Lagrangian at a high energy scale that is invariant under a flavor symmetry G_f , which is spontaneously broken by either the VEV

of a flavon field in the traditional flavor symmetry approach, or by the VEV of a modular field in the modular symmetry approach. In both approaches, the residual symmetries after symmetry breaking, denoted as G_ℓ and G_ν respectively in the charged lepton and neutrino sectors, are usually subgroups of G_f ⁵.

At the low energy scale, the effective Lagrangian of charged lepton and neutrino mass terms with a spontaneously broken G_f can be expressed as

$$-\mathcal{L}_{\text{mass}} = \overline{\ell_L} M_\ell \ell_R + \frac{1}{2} \overline{\nu_L} M_\nu \nu_L^c + \text{h.c.}, \quad (8)$$

where it is assumed that neutrinos are Majorana particles.

The residual symmetries G_ℓ and G_ν ensure that the operators $\overline{\ell_L} M_\ell \ell_R$ and $\overline{\nu_L} M_\nu \nu_L^c$ should be invariant under the transformation of $g_\ell \in G_\ell$ in the charged lepton sector and $g_\nu \in G_\nu$ in the neutrino sector, respectively. In the charged lepton sector, left-handed and right-handed charged leptons in their flavor space transform as $\ell_L \rightarrow \rho_L(g_\ell) \ell_L$, $\ell_R \rightarrow \rho_R(g_\ell) \ell_R$ under g_ℓ , leading to the mass term transforming as $\overline{\ell_L} M_\ell \ell_R \rightarrow \overline{\ell_L} \rho_L^\dagger(g_\ell) M_\ell \rho_R(g_\ell) \ell_R$, where $\rho_L(g_\ell)$ and $\rho_R(g_\ell)$ are representation matrices of g_ℓ in the basis of ℓ_L and ℓ_R , respectively. The invariance of the mass term under G_ℓ thus implies

$$\rho_L^\dagger(g_\ell) M_\ell \rho_R(g_\ell) = M_\ell. \quad (9)$$

It is convenient to introduce a Hermitian matrix $H_\ell = M_\ell M_\ell^\dagger$ to avoid unphysical rotation in the flavor space of right-handed charged leptons, whose invariance implies

$$\rho_L^\dagger(g_\ell) H_\ell \rho_L(g_\ell) = H_\ell. \quad (10)$$

This condition transmits to the restriction on the unitary matrix U_ℓ diagonalizing H_ℓ , $U_\ell^\dagger H_\ell U_\ell = \hat{H}_\ell \equiv \text{diag}\{m_e^2, m_\mu^2, m_\tau^2\}$,

$$\hat{H}_\ell [U_\ell^\dagger \rho_L(g_\ell) U_\ell] = [U_\ell^\dagger \rho_L U_\ell] \hat{H}_\ell. \quad (11)$$

In order to recover non-degenerate charged lepton masses, $U_\ell^\dagger \rho_L(g_\ell) U_\ell$ must be diagonal

$$U_\ell^\dagger \rho_L(g_\ell) U_\ell = \text{diag}\{e^{i\alpha_1}, e^{i\alpha_2}, e^{i\alpha_3}\}. \quad (12)$$

Therefore, G_ℓ must be an Abelian symmetry and the values of phases α_i (for $i = 1, 2, 3$) depend on which residual symmetry is selected.

In the neutrino sector, the invariance of $\overline{\nu_L} M_\nu \nu_L^c$ under the transformation $\nu_L \rightarrow \rho_L(g_\nu) \nu_L$ requires

$$\rho_L^\dagger(g_\nu) M_\nu \rho_L^*(g_\nu) = M_\nu \quad (13)$$

Similarly, given a unitary U_ν to diagonalize M_ν , $U_\nu^\dagger M_\nu U_\nu^* = \hat{M}_\nu \equiv \text{diag}\{m_1, m_2, m_3\}$, The above equation is rewritten as

$$\hat{M}_\nu [U_\nu^\dagger \rho_L(g_\nu) U_\nu]^* = [U_\nu^\dagger \rho_L(g_\nu) U_\nu] \hat{M}_\nu \quad (14)$$

⁵In a realistic model, sometimes the residual symmetries also include some additional accidental symmetries, but will not be considered in this work

The condition requires $[U_\nu^\dagger \rho_L(g_\nu) U_\nu]$ to be real and diagonal, and thus the only choices could be

$$[U_\nu^\dagger \rho_L(g_\nu) U_\nu] = \text{diag}\{(-1)^{k_1}, (-1)^{k_2}, (-1)^{k_3}\}. \quad (15)$$

where $k_{1,2,3} = 0, 1$. This conclusion leaves only Z_2 or $Z_2 \times Z'_2$ allowed as residual symmetry in the neutrino sector for Majorana neutrinos. Gathering together, Eqs. (12) and (15) leads to the partial dependence of U_ℓ and U_ν upon $\rho_L(g_\ell)$ and $\rho_L(g_\nu)$, and eventually results in the restriction on the leptonic mixing matrix $U_{\text{PMNS}} = U_\ell^\dagger U_\nu$. It is convenient to choose a flavour basis that $\rho_L(g_\ell)$ is diagonal, then U_ℓ is also diagonal and U_{PMNS} appears to be the unitary matrix to diagonalize $\rho_L(g_\nu)$,

$$U_{\text{PMNS}}^\dagger \rho_L(g_\nu) U_{\text{PMNS}} = \text{diag}\{(-1)^{k_1}, (-1)^{k_2}, (-1)^{k_3}\}. \quad (16)$$

With the help of residual symmetries, we further show in detail the realization of TM_1 mixing pattern from residual symmetries of S_4 . S_4 is the permutation group of four objects, which is also isomorphic to the octahedral group. It has 24 elements, generated by three generators satisfying [17]

$$S^2 = T^3 = U^2 = (ST)^3 = (SU)^2 = (TU)^2 = (STU)^4 = I, \quad (17)$$

where T is a order-3 generator, and S and U are order-2 generators. The group has two irreducible 3-dimensional representations **3** and **3'**, in which T , S and U are represented as

$$\rho_{\mathbf{3}^{(\prime)}}(T) = \begin{pmatrix} 1 & 0 & 0 \\ 0 & \omega^2 & 0 \\ 0 & 0 & \omega \end{pmatrix}, \quad \rho_{\mathbf{3}^{(\prime)}}(S) = \frac{1}{3} \begin{pmatrix} -1 & 2 & 2 \\ 2 & -1 & 2 \\ 2 & 2 & -1 \end{pmatrix}, \quad \rho_{\mathbf{3}, \mathbf{3}'}(U) = \pm \begin{pmatrix} 1 & 0 & 0 \\ 0 & 0 & 1 \\ 0 & 1 & 0 \end{pmatrix}, \quad (18)$$

where a basis of diagonal T has been chosen [30]. The symmetry $Z_3^T = \{I, T, T^2\}$ is chosen as the residual symmetry in the charged lepton sector to guarantee a diagonal H_l . Then, the mixing matrix is only determined by the residual symmetry G_ν in the neutrino sector. There could be a few choices on the possible G_ν , such as:

- Taking G_ν to be $Z_2^S = \{I, S\}$, diagonalizing $\rho_{\mathbf{3}^{(\prime)}}(S)$ fixes the second row of $|U_{\text{TBM}}|$, i.e., TM_2 mixing. The first and third row cannot be fixed since both of them refers to the degenerate eigenvalue -1 of $\rho_{\mathbf{3}^{(\prime)}}(S)$. Realization of the pattern requires only a A_4 symmetry since the generator U is not necessary. Realizations in modular A_4 symmetries are presented in [33, 34].
- Taking $Z_2^U = \{I, U\}$, diagonalizing $\rho_{\mathbf{3}^{(\prime)}}(U)$ fixes the third row of $|U_{\text{TBM}}|$, leading to $\theta_{13} = 0$ and $\theta_{23} = 45^\circ$. This case has already been excluded.
- The third choice is to take G_ν to be $Z_2^{SU} = \{I, SU\}$. Here representation matrices of SU in **3** and **3'** are explicitly written as

$$\rho_{\mathbf{3}, \mathbf{3}'}(SU) = \pm \frac{1}{3} \begin{pmatrix} -1 & 2 & 2 \\ 2 & 2 & -1 \\ 2 & -1 & 2 \end{pmatrix}. \quad (19)$$

The vector $(2, -1, -1)$ is the eigenvector respecting the non-degenerate eigenvalue of $\rho_{\mathbf{3}, \mathbf{3}'}(SU)$. Therefore, TM_1 is achieved once the residual symmetry is Z_2^{SU} .

The prediction of TM_1 mixing pattern is thus obtained via the structure of residual symmetries assigned as $G_\ell = Z_3^T$ and $G_\nu = Z_2^{SU}$, which is independent of model details and regardless of realizations in traditional flavor symmetry or modular symmetry.

3 Models based on modular S_4 symmetry

In this paper, we assume a modular S_4 symmetry present in the lepton sector at a very high energy scale to account for the trimaximal mixing patterns in the lepton mass matrices, which is spontaneously broken to some residual symmetries by either the VEV of the modular field τ or a triplet flavon field φ . We will first review the necessary ingredients needed for model building based on modular S_4 symmetry, and then follow the approaches given in the Figure 1 to construct explicit models featuring TM_1 mixing.

Let us begin with the definition of modular S_4 symmetry following [29,30,35]. A modular group $\bar{\Gamma}$ is the group of linear fraction transformations acting on the complex modulus τ in the upper half complex plane ($\text{Im}(\tau) > 0$):

$$\tau \rightarrow \gamma\tau = \frac{a\tau + b}{c\tau + d}, \quad (20)$$

with $a, b, c, d \in \mathbb{Z}$ and $ad - bc = 1$. When representing each element of $\bar{\Gamma}$ by a two by two matrix, $\bar{\Gamma}$ can be expressed as

$$\bar{\Gamma} = \left\{ \begin{pmatrix} a & b \\ c & d \end{pmatrix} / (\pm \mathbf{1}), a, b, c, d \in \mathbb{Z}, ad - bc = 1 \right\}. \quad (21)$$

The modular group is isomorphic to the projective special linear group $PSL(2, \mathbb{Z}) = SL(2, \mathbb{Z})/Z_2$, and possesses two generators $S_\tau : \tau \rightarrow -1/\tau$ and $T_\tau : \tau \rightarrow \tau + 1$ satisfying $S_\tau^2 = (S_\tau T_\tau)^3 = \mathbf{1}$. By requiring $a, d = 1 \pmod{N}$ and $b, c = 0 \pmod{N}$ with $N = 2, 3, 4, \dots$, we can get a subset as

$$\bar{\Gamma}(N) = \left\{ \begin{pmatrix} a & b \\ c & d \end{pmatrix} / \in PSL(2, \mathbb{Z}), \begin{pmatrix} a & b \\ c & d \end{pmatrix} = \begin{pmatrix} 1 & 0 \\ 0 & 1 \end{pmatrix} \pmod{N} \right\}. \quad (22)$$

The quotient group $\bar{\Gamma}/\bar{\Gamma}(N)$ can then be defined as the finite modular group Γ_N , which can be obtained by imposing a constraint $T_\tau^N = 1$ in addition to $S_\tau^2 = (S_\tau T_\tau)^3 = \mathbf{1}$. The finite modular group Γ_N is isomorphic to a permutation group. In particular, it was shown that $\Gamma_2 \simeq S_3$, $\Gamma_3 \simeq A_4$, $\Gamma_4 \simeq S_4$ for $N = 2, 3, 4$ [36].

For our purpose, we only care about the modular group S_4 satisfying $S_\tau^2 = (S_\tau T_\tau)^3 = T_\tau^4 = \mathbf{1}$. In literature it is more common to use Eq. (17) to generate the group S_4 , which relates to the generators of the finite modular group $\Gamma(N)$ as:

$$S = T_\tau^2, \quad T = S_\tau T_\tau, \quad U = T_\tau S_\tau T_\tau^2 S_\tau. \quad (23)$$

The CG coefficient of the S_4 group is listed in the Appendix of [30].

In the upper complex plane with the requirement $\tau = \tau + 4$, the generators S , T , and U can be represented by 2×2 matrices which are not unique due to the identification. For later convenience, we only list the representations of T and SU here [29, 30]

$$T = \begin{pmatrix} 0 & 1 \\ -1 & -1 \end{pmatrix}, \quad SU = \begin{pmatrix} -1 & -1 \\ 2 & 1 \end{pmatrix}. \quad (24)$$

If a modulus τ_0 is invariant under a nontrivial $SL(2, \mathbb{Z})$ transformation $\gamma_0 \neq I$, then this modulus τ_0 is known as a fixed point which gives $\gamma\tau_\gamma = \tau_\gamma$, with γ known as a stabilizer of

τ_γ . For the γ generated by the representations given in Eq. (24), it is straightforward to compute the fixed points:

$$\tau_T = \omega = -\frac{1}{2} + i\frac{\sqrt{3}}{2}, \tau_{SU} = -\frac{1}{2} + \frac{i}{2}, \quad (25)$$

Under the modular invariance Γ_N , a chiral superfield $\phi_i(\tau)$ transforms non-linearly as function of τ as

$$\phi_i(\tau) \rightarrow \phi_i(\gamma\tau) = (c\tau + d)^{-2k_i} \rho_{I_i}(\gamma) Y_{I_Y}(\tau), \quad (26)$$

Due to the holomorphicity of the superpotential, the Yukawa coupling transforms as:

$$Y_{I_Y}(\tau) \rightarrow Y_{I_Y}(\gamma\tau) = (c\tau + d)^{2k_Y} \rho_{I_Y}(\gamma) Y_{I_Y}(\tau), \quad (27)$$

where k_Y must be non-negative.

Once the modular field gains a VEV at such a stabiliser, an Abelian residual modular symmetry generated by is preserved.

If the modular field τ acquire a VEV at a fixed point such that $\langle \tau \rangle = \tau_\gamma$, an Abelian residual symmetry generated by γ is preserved leaving $Y_I(\gamma\tau_\gamma) = Y_I(\tau_\gamma)$, and thus a characteristic equation can be written

$$\rho_I(\gamma) Y_I(\tau_\gamma) = (c\tau + d)^{-2k} Y_I(\tau_\gamma), \quad (28)$$

with the eigenvalues $(c\tau + d)^{-2k}$ for the representation matrix $\rho_I(\gamma)$ [35, 37]. Now, given a representation matrix of S_4 , it is straightforward to use the above equation to determine the eigenvectors for the modular form $Y_I(\tau_\gamma)$. For example, at the fixed point $\tau_\gamma = \tau_T$, the modular forms are [29, 30]:

$$Y_{\mathbf{3}'}^{(6j+2)}(\tau_T) \propto \begin{pmatrix} 0 \\ 1 \\ 0 \end{pmatrix}, \quad Y_{\mathbf{3}'}^{(6j+4)}(\tau_T) \propto \begin{pmatrix} 0 \\ 0 \\ 1 \end{pmatrix}, \quad Y_{\mathbf{3}'}^{(6j+6)}(\tau_T) \propto \begin{pmatrix} 1 \\ 0 \\ 0 \end{pmatrix}, \quad (29)$$

where j is a non-negative integer.

Similarly, at the fixed point $\tau_\gamma = \tau_{SU}$, one can solve for the eigenvector of $\rho_{\mathbf{3}'}(SU)$ with respect to the degenerate eigenvalue 1, to obtain the modular forms with weight ≤ 4 to be

$$\begin{aligned} Y_{\mathbf{2}}^{(2)}(\tau_{SU}) &\propto \begin{pmatrix} 1 \\ -1 \end{pmatrix}, & Y_{\mathbf{3}'}^{(2)}(\tau_{SU}) &\propto \begin{pmatrix} 1 \\ 1 - \sqrt{6} \\ 1 + \sqrt{6} \end{pmatrix}, \\ Y_{\mathbf{3}'}^{(4)}(\tau_{SU}) &\propto \begin{pmatrix} 2 \\ -1 \\ -1 \end{pmatrix}, & Y_{\mathbf{3}}^{(4)}(\tau_{SU}) &\propto \begin{pmatrix} \sqrt{2} \\ \sqrt{2} - \sqrt{3} \\ \sqrt{2} + \sqrt{3} \end{pmatrix}. \end{aligned} \quad (30)$$

With the above knowledge at hand, we can build concrete models based on modular S_4 symmetry. Assuming that at low energy, the charged lepton sector and the neutrino sector have different residual flavor symmetries G_ℓ and G_ν , respectively, as was discussed in Section 2.2, there can be three approaches to do model building as shown in 1: 1) the symmetry of charged lepton sector is broken down to a Z_3^T residual symmetry by a flavon φ_ℓ , while the residual symmetry in neutrino sector is a Z_2^{SU} guaranteed by the VEV of modular field τ_ν ; 2) the symmetry of charged lepton sector is broken down to a Z_3^T

residual symmetry due to the modular field τ_l , while a Z_2^{SU} residual symmetry remains in the neutrino sector due to the VEVs of flavons φ_ν that only couple to neutrinos; 3) the sectors of charged leptons and neutrinos are dependent on two different modular fields, and the final trimaximal mixing pattern is achieved by choosing specific VEVs for the modular fields. In the following subsections, we will proceed with analyzing three different models explicitly with the mentioned approaches, and see how they result in similar neutrino mass matrices and phenomenology.

3.1 Model A

The first model realizing the TM_1 mixing from modular S_4 symmetry can be achieved by adding flavons in the lepton sector which breaks the flavor symmetry to a residual Z_3^T symmetry, and an additional modular field τ_ν in the neutrino sector which stabilizes at $\langle \tau_\nu \rangle = \tau_{SU}$ to ensure a residual Z_2 symmetry. In this case, all couplings of neutrinos can be promoted to modular forms, making the neutrino sector look more elegant.

However, it is not that easy to construct a realistic model along this approach because of two reasons. Firstly, there are only two flavor singlets under S_4 , either **1** or **1'**, so it is hard to embed three right-handed charged leptons within the two non-degenerate flavor singlets, unless extra symmetry like a Z_n is introduced to separate the charged leptons. This problem may be avoided by introducing a modular weight to one of the degenerate charged leptons, but Z_n charges are still needed if one requires the absence of trivial neutrino mass terms. Secondly, the contraction between a flavon $\varphi_\ell \sim \mathbf{3}$ and left-handed charged leptons $L \sim \mathbf{3}$ cannot contract with the singlet **1'** as the decomposition of representation products gives: $\mathbf{3} \times \mathbf{3} \rightarrow \mathbf{1} + \mathbf{2} + \mathbf{3} + \mathbf{3}'$. This means that we need to introduce extra flavons like $\eta \sim \mathbf{2}$ to make them contractible. These couplings will inevitably be higher-order operators as can be checked from the superpotential in Eq. (31). To cancel all lower-order couplings while keeping all the first three terms in Eq. (31), there will be a constraint on the charge of the discrete symmetry Z_n .

Fermions	S_4	$2k$	Scalars	S_4	$2k$	Modular forms	S_4	$2k$
e^c	1	-3	φ_ℓ	3	+2	$Y_{\mathbf{2}}(\tau_\nu)$	2	+2
μ^c	1'	-2	η	2	-1	$Y_{\mathbf{3}'}(\tau_\nu)$	3'	+2
τ^c	1	-2	ξ	1'	+1			
L	3	+1	$H_{u,d}$	1	0			
ν^c	3	-1						

Table 1: Lepton and Higgs superfields.

We can still try to write down a simple toy model by assuming that all appropriate Z_n charges are assigned to the superfields so that couplings giving the masses of charged leptons are provided by the first line of the following superpotential:

$$\begin{aligned}
W = & \frac{y_e \xi^3}{\Lambda^4} (L \varphi_\ell)_{\mathbf{1}'} e^c H_d + \frac{y_\mu}{\Lambda^2} (L (\varphi_\ell \eta)_{\mathbf{3}'})_{\mathbf{1}'} \mu^c H_d + \frac{y_\tau}{\Lambda^2} (L (\varphi_\ell \eta)_{\mathbf{3}})_{\mathbf{1}} \tau^c H_d \\
& + y_D(\tau_\nu) L \nu^c H_u + \frac{1}{2} Y_{\mathbf{2}}(\tau_\nu) (\nu^c \nu^c)_{\mathbf{2}} \xi + \frac{1}{2} Y_{\mathbf{3}'}(\tau_\nu) (\nu^c \nu^c)_{\mathbf{3}} \xi. \tag{31}
\end{aligned}$$

where L is the left-handed charged lepton doublets, e^c, μ^c, τ^c are right-handed charged leptons, ν^c are right-handed neutrinos, and a few flavons $\varphi_\ell, \eta, \xi, \xi'$ are introduced to make

them contractible. The VEV of flavons contracted with leptons should acquire the VEVs along $\langle \varphi_\ell \rangle = v_{\varphi_\ell}(1, 0, 0)^T$, $v_\eta = (v_{\eta_1}, v_{\eta_2})^T$ to preserve the residual Z_3^T symmetry in the charged lepton sector. Meanwhile, in the neutrino sector, the VEV of the modular field τ_ν is fixed at $\langle \tau_\nu \rangle = \tau_{SU} = -\frac{1}{2} + \frac{i}{2}$ to preserve the residual Z_2^{SU} symmetry. The CG coefficients for S_4 are given in the Appendix A of [30] when expanding the contractions.

In the charged lepton sector, the Yukawa matrix includes a $\mu - \tau$ mixing as

$$M_\ell^* = \frac{v_d v_{\varphi_\ell}}{\Lambda^2} \begin{pmatrix} \frac{y_e v_\xi^3}{\Lambda^2} & 0 & 0 \\ 0 & y_\mu v_{\eta_1} & y_\tau v_{\eta_1} \\ 0 & -y_\mu v_{\eta_2} & y_\tau v_{\eta_2} \end{pmatrix}. \quad (32)$$

where $v_d = \langle H_d \rangle$, and the charged lepton mass matrix is defined in the left-right convention to be consistent with the convention used in Eq. (8), which gives an an additional complex conjugation [38]. Thus, a unitary matrix U_ℓ

$$U_\ell = \begin{pmatrix} e^{-i\alpha'_3} & 0 & 0 \\ 0 & \cos \theta_\ell e^{i\alpha_1} & \sin \theta_\ell e^{-i\alpha_2} \\ 0 & -\sin \theta_\ell e^{i\alpha_2} & \cos \theta_\ell e^{-i\alpha_1} \end{pmatrix} \quad (33)$$

should be included to diagonalize $M_\ell M_\ell^\dagger$.

In the neutrino sector, the Dirac mass matrix in the flavor basis, i.e., basis of charge lepton mass eigenstates, is given simply by

$$M_D = y_D^* v_u U_\ell^\dagger \begin{pmatrix} 1 & 0 & 0 \\ 0 & 0 & 1 \\ 0 & 1 & 0 \end{pmatrix}, \quad (34)$$

where $v_u \equiv \langle H_u \rangle$, and U_ℓ^\dagger is inserted to diagonalize the charged leptons.

When considering the Majorana neutrino mass matrix, we start with the simplest case by including only weight-2 modular forms, $Y_{\mathbf{2}}(\tau_\nu) \sim \mathbf{2}$ and $Y_{\mathbf{3}'}(\tau_\nu) \sim \mathbf{3}'$. Apparently, making the modular weights higher than 2 will increase the number of free parameters that will fit with the data eventually, which is the reason why we only check how the model can be built with the least number of free parameters. Using Eq. (30) where $Y_{\mathbf{2}}(\tau_{SU}) \propto (1, -1)^T$ and $Y_{\mathbf{3}'}(\tau_{SU}) \propto (1, 1 - \sqrt{6}, 1 + \sqrt{6})^T$ for the weight $2k_\nu = 2$, the Majorana mass matrix is

$$M_R^* = \begin{pmatrix} 0 & -Y_{\mathbf{2},1} & Y_{\mathbf{2},2} \\ -Y_{\mathbf{2},1} & Y_{\mathbf{2},2} & 0 \\ Y_{\mathbf{2},2} & 0 & -Y_{\mathbf{2},1} \end{pmatrix} + \begin{pmatrix} 2Y_{\mathbf{3}',1} & -Y_{\mathbf{3}',2} & -Y_{\mathbf{3}',3} \\ -Y_{\mathbf{3}',2} & 2Y_{\mathbf{3}',3} & -Y_{\mathbf{3}',1} \\ -Y_{\mathbf{3}',3} & -Y_{\mathbf{3}',1} & 2Y_{\mathbf{3},2} \end{pmatrix}. \quad (35)$$

It is more convenient to re-parameterize the above Majorana mass matrix into the following form:

$$M_R = a_2 \begin{pmatrix} 0 & 1 & 1 \\ 1 & 1 & 0 \\ 1 & 0 & 1 \end{pmatrix} + a_3 \begin{pmatrix} 2 & -1 & -1 \\ -1 & 2 & -1 \\ -1 & -1 & 2 \end{pmatrix} - a_3 \sqrt{6} \begin{pmatrix} 0 & 1 & -1 \\ 1 & 2 & 0 \\ -1 & 0 & -2 \end{pmatrix}, \quad (36)$$

where $a_2 = [\lambda_2 Y_{\mathbf{2},1}^{(2)}(\tau_{SU})]^*$, $a_3 = [\lambda_3 Y_{\mathbf{3}',1}^{(2)}(\tau_{SU})]^*$ are complex coefficients.

Finally, by applying the standard neutrino seesaw formula

$$M_\nu = -M_D M_R^{-1} M_D^T, \quad (37)$$

it is straightforward to compute the mass matrix for the active neutrinos and then proceed with the diagonalization to find the PMNS matrix, which will be discussed in details in the next section.

3.2 Model B

An alternative approach to the previous scenario is to use the VEV of the modular field to achieve Z_3^T in the charged lepton sector, and then introduce additional flavons in the neutrino sector to break to the residual Z_2^{SU} symmetry. This scenario should be similar to the method discussed in [39]. The superfield assignments of Model B are listed in the Table 2.

Fermions	S_4	$2k$	Scalars	S_4	$2k$	Modular forms	S_4	$2k$
e^c	1'	-6	φ_ν	3	0	$Y_e(\tau_l)$	3'	+6
μ^c	1'	-4	φ'_ν	3'	0	$Y_\mu(\tau_l)$	3'	+4
τ^c	1'	-2	η	1'	0	$Y_\tau(\tau_l)$	3'	+2
L	3	0	$H_{u,d}$	1	0	y_D	1	0
ν^c	3	0						

Table 2: The superfields, Yukawa couplings and masses with different representations and weights in Model B.

The superpotential that is invariant under this superfield assignment is:

$$\begin{aligned} W = & Y_e(\tau_l) L e^c H_d + Y_\mu(\tau_l) L \mu^c H_d + Y_\tau(\tau_l) L \tau^c H_d \\ & + y_D (L \nu^c) \mathbf{1} H_u + \frac{1}{2} M_1 (\nu^c \nu^c) \mathbf{1} + \lambda \varphi_\nu (\nu^c \nu^c) \mathbf{3} + \frac{1}{\Lambda} \lambda' \varphi'_\nu (\nu^c \nu^c \eta) \mathbf{3}' . \end{aligned} \quad (38)$$

When the VEV of modular field is set to the fixed point τ_T , the leptons will be put into the AF basis [30], implying

$$Y_e(\tau_T) \propto \begin{pmatrix} 1 \\ 0 \\ 0 \end{pmatrix}, \quad Y_\mu(\tau_T) \propto \begin{pmatrix} 0 \\ 0 \\ 1 \end{pmatrix}, \quad Y_\tau(\tau_T) \propto \begin{pmatrix} 0 \\ 1 \\ 0 \end{pmatrix}, \quad (39)$$

so that the lepton mass matrix is diagonal.

In the neutrino sector, the Dirac neutrino mass matrix has the same form as in Eq. (34). In the Majorana terms, the right-handed neutrino triplets $(\nu^c \nu^c)$ in this model should be contracted following the S_4 product rule $\mathbf{3} \times \mathbf{3} = \mathbf{1} + \mathbf{2} + \mathbf{3} + \mathbf{3}'$. However, as shown in [39], if we have only one flavon field which is a triplet **3** of S_4 , the deduced Majorana mass matrix leads to only a tri-bimaximal mixing with $\theta_{13} = 0$ predicted. Therefore, an economical choice is to introduce only two flavons in either a **3** or a **3'** representation of S_4 . To preserve the residual symmetry of Z_2^{SU} , one must have the VEV of these flavons aligned as:

$$\langle \varphi_\nu \rangle = v_{SU} \begin{pmatrix} 1 \\ 1 \\ 1 \end{pmatrix}, \quad \langle \varphi'_\nu \rangle = v'_{SU} \begin{pmatrix} 0 \\ 1 \\ -1 \end{pmatrix}. \quad (40)$$

Expanding the superpotential, the Majorana mass matrix for the right-handed neutrinos now reads

$$M_R = b_1 \begin{pmatrix} 1 & 0 & 0 \\ 0 & 0 & 1 \\ 0 & 1 & 0 \end{pmatrix} + b_2 \begin{pmatrix} 2 & -1 & -1 \\ -1 & 2 & -1 \\ -1 & -1 & 2 \end{pmatrix} + b_3 \begin{pmatrix} 0 & 1 & -1 \\ 1 & 2 & 0 \\ -1 & 0 & -2 \end{pmatrix}, \quad (41)$$

where $b_1 = M_1^*$, $b_2 = (\lambda v_{SU})^*$ and $b_3 = (\frac{1}{\Lambda} \lambda' v'_{SU})^*$. Due to the suppression of higher-dimensional operator, b_3 is in general much smaller than b_2 . Similar to Model A, the complex conjugate appears because of a matching to the M_R defined in the left-right convention. To this point, all the mass matrices have been written so the seesaw equation Eq. (37) can be applied again to find the mass matrix for the active neutrinos.

3.3 Model C

The previous two scenarios contain only one modular field in either the lepton or the neutrino sector, and a few flavons with particular VEVs alignment to obtain the desired residual symmetry. It is also possible to use two modular fields in both the lepton and the neutrino sector, so that all Yukawa couplings can be expressed as non-trivial modular forms. The generalization from one modulus to multiple moduli was given in [29,30], where a bi-triplet flavon Φ was introduced to break the modular $S_4^l \times S_4^\nu$ symmetry down to a diagonal S_4 subgroup through the VEV of Φ . The two modular fields can get different VEVs at different fixed points which then result in different residual symmetries in the lepton or neutrino sectors. A minimal model realizing the above picture requires the superfields to be assigned according to Table. 3 [30].

Fields	S_4^l	S_4^ν	$2k_l$	$2k_\nu$
e^c	1'	1	-6	-2
μ^c	1'	1	-4	-2
τ^c	1'	1	-2	-2
L	3	1	0	+2
ν^c	1	3	0	-2
Φ	3	3	0	0
$H_{u,d}$	1	1	0	0

Table 3: Lepton and Higgs superfields in scenario 3.

The superpotential for these superfields is given by:

$$W = Y_e(\tau_T) L e^c H_d + Y_\mu(\tau_T) L \mu^c H_d + Y_\tau(\tau_T) L \tau^c H_d + \frac{y_\nu}{\Lambda} L \Phi H_u \nu^c + \frac{1}{2} M_1(\tau_\nu) (\nu^c \nu^c)_{\mathbf{1}} + \frac{1}{2} M_2(\tau_\nu) (\nu^c \nu^c)_{\mathbf{2}} + \frac{1}{2} M_3(\tau_\nu) (\nu^c \nu^c)_{\mathbf{3}}. \quad (42)$$

This scenario gives the same Yukawa matrices for charged leptons and thus will not be repeated.

In the neutrino sector, the Dirac masses for the right-handed neutrinos are given by the non-renormalizable operator proportional to a modulus-independent coefficient y_ν . The symmetry breaking $S_4^l \times S_4^\nu \rightarrow S_4$ is naturally achieved via the VEV of a bi-triplet scalar field $\Phi \sim (\mathbf{3}, \mathbf{3})$ of $S_4^l \times S_4^\nu$. By minimizing the superpotential, the scalar gains a VEV along the direction of $\langle \Phi \rangle_{\alpha i} = v_\Phi (P_{23})_{\alpha i}$ with

$$P_{23} = \begin{pmatrix} 1 & 0 & 0 \\ 0 & 0 & 1 \\ 0 & 1 & 0 \end{pmatrix}. \quad (43)$$

Expanding the Dirac Yukawa coupling $\frac{y_\nu}{\Lambda} L \Phi H_u \nu^c$ after the breaking of $S_4^l \times S_4^\nu \rightarrow S_4$ and the Higgs H_u acquiring a VEV, we get

$$M_D = y_D^* P_{23} v_u, \quad \text{with} \quad y_D = \frac{y_\nu v_\Phi}{\Lambda}. \quad (44)$$

The Majorana neutrino sector includes three modulus-dependent couplings $M_{\mathbf{r}}(\tau_\nu)$ with $\mathbf{r} = \mathbf{1}, \mathbf{2}, \mathbf{3}$ that in general give a Majorana mass matrix with the following form⁶:

$$M_R^* = \begin{pmatrix} M_{\mathbf{1}} & 0 & 0 \\ 0 & 0 & M_{\mathbf{1}} \\ 0 & M_{\mathbf{1}} & 0 \end{pmatrix} + \begin{pmatrix} 0 & M_{\mathbf{2},1} & M_{\mathbf{2},2} \\ M_{\mathbf{2},1} & M_{\mathbf{2},2} & 0 \\ M_{\mathbf{2},2} & 0 & M_{\mathbf{2},1} \end{pmatrix} + \begin{pmatrix} 2M_{\mathbf{3},1} & -M_{\mathbf{3},3} & -M_{\mathbf{3},2} \\ -M_{\mathbf{3},3} & 2M_{\mathbf{3},2} & -M_{\mathbf{3},1} \\ -M_{\mathbf{3},2} & -M_{\mathbf{3},1} & 2M_{\mathbf{3},3} \end{pmatrix}. \quad (45)$$

Assuming that the modular field τ_ν is fixed at the fixed point $\langle \tau_\nu \rangle = \tau_{SU}$, we can use the modular forms given in Eq. (30) to rewrite the Majorana mass matrix M_R , and then parameterize it into the following form [30]:

$$M_R = c_1 \begin{pmatrix} 1 & 0 & 0 \\ 0 & 0 & 1 \\ 0 & 1 & 0 \end{pmatrix} + c_2 \begin{pmatrix} 0 & 1 & 1 \\ 1 & 1 & 0 \\ 1 & 0 & 1 \end{pmatrix} + c_3 \sqrt{2} \begin{pmatrix} 2 & -1 & -1 \\ -1 & 2 & -1 \\ -1 & -1 & 2 \end{pmatrix} - c_3 \sqrt{3} \begin{pmatrix} 0 & 1 & -1 \\ 1 & 2 & 0 \\ -1 & 0 & -2 \end{pmatrix}, \quad (46)$$

where $c_1 = [M_{\mathbf{1}}(\tau_{SU})]^*$, $c_2 = [M_{\mathbf{2},1}(\tau_{SU})]^*$ and $c_3 = \frac{1}{\sqrt{2}}[M_{\mathbf{3},1}(\tau_{SU})]^*$.

Thus the active neutrino mass matrix becomes

$$M_\nu = -M_D M_R^{-1} M_D^T = -(y_D^*)^2 v_u^2 P_{23} M_R^{-1} P_{23}. \quad (47)$$

4 Fit with JUNO Data

4.1 Parameterization

With the lepton and neutrino mass matrices given in the above models, it is now straightforward to compute the experimental predictions for Majorana mass matrices and mixings. In particular, since all three models exhibit a similarity in their mass matrices, it is convenient to first put them into a block diagonal form by applying a TBM mixing matrix,

$$U_{\text{TBM}}^T M_R U_{\text{TBM}} = \begin{pmatrix} \eta & 0 & 0 \\ 0 & \alpha & \gamma \\ 0 & \gamma & \beta \end{pmatrix}, \quad (48)$$

where it can be shown that

Model A : $\eta = -\alpha + \beta$, $\gamma = \alpha - 2\beta$, with $\alpha = 2a_2$, $\beta = a_2 + 3a_3$,

Model B : $\eta = 2\alpha + \beta$, with $\alpha = b_1$, $\beta = -b_1 + 3b_2$, $\gamma = \sqrt{6}b_3$,

Model C : $\eta = -\beta - 2\gamma$, with $\alpha = c_1 + 2c_2$, $\beta = -c_1 + c_2 + 3\sqrt{2}c_3$, $\gamma = -3\sqrt{2}c_3$,

where the parameters a_i , b_i , and c_i with $i = 1, 2, 3$ are free parameters defined for Models A, B, and C in Eqs. (36), (41), (46), respectively. Therefore, we can always simplify the computation by re-parameterizing those free parameters in the original M_R into the above

⁶Note that there are no $M_{\mathbf{3}'}$ term since it vanishes because of its antisymmetric nature.

form with either two complex parameters (α, β for Model A), or three complex parameters (α, β, γ for Models B and C).

On the other hand, the Dirac mass matrix takes a similar form except an unitary matrix U_ℓ particularly for Model A in the charged lepton flavor basis. Using the type-I seesaw formula in eq. (37), we can write

$$M_\nu = -m_0^2 U_\ell^\dagger P_{23} M_R^{-1} P_{23}^T U_\ell^*. \quad (49)$$

with an overall factor $m_0^2 = (y_D^*)^2 v_u^2$.

By the PMNS matrix defined as $U_{\text{PMNS}} = U_\ell^\dagger U_{\text{TM}_1}$ with U_ℓ the matrix diagonalizing charged leptons defined in Eq. (33), we can diagonalize M_ν which gives the eigenvalues of light neutrino masses. In particular, we found a strong correlation between the mixing angle $\sin \theta_{13}$ and the three eigenvalues of neutrino mass matrix:

$$\begin{aligned} 1 + \frac{11}{8} \cos^2(2\theta_R) + \cos(2\theta_R) \frac{(5m_1^2 m_3^2 - 4m_2^2 m_3^2 + 5m_1^2 m_2^2)}{4\Delta m_{23}^2 m_1^2} \\ = \frac{13}{8} \frac{m_2^2 + m_3^2}{\Delta m_{23}^2} + \frac{m_2^2 m_3^2}{m_1^2} \frac{(50m_3^2 - 17\Delta m_{23}^2)}{(\Delta m_{23}^2)^2}. \end{aligned} \quad (50)$$

However, after numerical trial, we can not find an existing parameter space for Model A because it is over-constrained as we only have 2 free parameters in the Majorana mass matrix. As mentioned in Section 3.1, modifying to higher modular weight of τ_ν , it is still possible to fit the data with the price of introducing more free parameters, rendering model A less predictive and thus will not be considered any more in this work.

In the rest of the section, we will concentrate on Models B and C. Without mixing in the charged lepton sector, the neutrino mass matrix can be diagonalized by the TM_1 matrix defined in Eq. (4) by definition:

$$U_{\text{TM}_1}^\dagger M_\nu U_{\text{TM}_1}^* = -m_0^2 \begin{pmatrix} \frac{1}{|\eta|} & 0 & 0 \\ 0 & e^{-2i\alpha_3} \left[V^\dagger \begin{pmatrix} \alpha & \gamma \\ \gamma & \beta \end{pmatrix} V^* \right]^{-1} & 0 \\ 0 & 0 & M_1^{-1} \end{pmatrix} \equiv -m_0^2 \begin{pmatrix} M_1^{-1} & & \\ & M_2^{-1} & \\ & & M_3^{-1} \end{pmatrix}, \quad (51)$$

where a phase factor of η can be extracted to reduce one free parameter, and the unitary matrix V is used to diagonalize the bottom-right block defined as

$$V \equiv e^{i\alpha_3} \begin{pmatrix} \cos \theta_R e^{-i\alpha_1} & \sin \theta_R e^{i\alpha_2} \\ \sin \theta_R e^{-i\alpha_2} & -\cos \theta_R e^{i\alpha_1} \end{pmatrix}. \quad (52)$$

Under this parameterization, the general form of U_{TM_1} can be expressed in terms of the TBM matrix defined in Eq. (3):

$$U_{\text{TM}_1} \equiv U_{\text{TBM}} \begin{pmatrix} e^{-i\alpha'_3} & 0 & 0 \\ 0 & \cos \theta_R e^{i\alpha_1} & \sin \theta_R e^{-i\alpha_2} \\ 0 & -\sin \theta_R e^{i\alpha_2} & \cos \theta_R e^{-i\alpha_1} \end{pmatrix}, \quad (53)$$

where $\alpha'_3 = \frac{1}{2}\arg(\eta)$.

As a result, the predictions of observables under the above parameterization, such as the mixing angles and the CP-violating phase, can be computed explicitly. Since an overall phase of γ can be dropped, there are at most five free parameters for all three proposed models to fit with the five observables in neutrino experiments such as three mixing angles and two mass differences.

4.2 Predictions of observables and sum rules

In Models B and C, it is possible to solve for the predictions of neutrino oscillation parameters analytically. The mixing angles and Dirac-type CP-violating phase under the above parameterization is given by [30]:

$$\begin{aligned}\sin \theta_{13} &= \frac{\sin \theta_R}{\sqrt{3}}, \\ \tan \theta_{12} &= \frac{\cos \theta_R}{\sqrt{2}}, \\ \tan \theta_{23} &= \left| \frac{\cos \theta_R + \sqrt{\frac{2}{3}} e^{i(\alpha_1 - \alpha_2)} \sin \theta_R}{\cos \theta_R - \sqrt{\frac{2}{3}} e^{i(\alpha_1 - \alpha_2)} \sin \theta_R} \right|, \\ \delta &= \arg[(5(\cos 2\theta_R + 1) \cos(\alpha_1 - \alpha_2) - i(\cos 2\theta_R + 5) \sin(\alpha_1 - \alpha_2))],\end{aligned}\quad (54)$$

These correlations recover sum rules between mixing angles and CP phase shown in Eq. (5).

The lightest eigenvalue of M_ν under this parameterization is given by $m_{\text{lightest}} = m_0^2/M_1$ for normal ordering (NO), and $m_{\text{lightest}} = m_0^2/M_3$ for inverted ordering (IO). Meanwhile, since M_1 is fixed by η which is dependent on α, β, γ in our models, there should be a correlation between M_1, M_2 and M_3 that can be solved by diagonalizing the bottom-right 2×2 block in Eq. (51). For Model B, $\eta = 2\alpha + \beta$ so we have:

$$\frac{1}{m_1} = \frac{1}{|2\alpha + \beta|} = \left| \frac{2 \cos^2 \theta_R e^{-2i\alpha_1} + \sin^2 \theta_R e^{-2i\alpha_2}}{m_2} + \frac{\cos^2 \theta_R e^{2i\alpha_1} + 2 \sin^2 \theta_R e^{2i\alpha_2}}{m_3} \right|. \quad (55)$$

For Model C, the correlation is different because now we have $\eta = -\beta - 2\gamma$:

$$\frac{1}{m_1} = \frac{1}{|\beta + 2\gamma|} = \left| \frac{\sin^2 \theta_R e^{2i\alpha_2} + \sin 2\theta_R e^{i(\alpha_1 + \alpha_2)}}{m_2} + \frac{\cos^2 \theta_R e^{-2i\alpha_1} - \sin 2\theta_R e^{-i(\alpha_1 + \alpha_2)}}{m_3} \right|. \quad (56)$$

Furthermore, the effective neutrino mass parameter m_{ee} in neutrinoless double beta decay experiments can also be solved for Model B

$$\begin{aligned}m_{ee} &= m_0^2 \left| M_{R,B(1,1)}^{-1} \right| = \left| \frac{2}{3(2\alpha + \beta)} + \frac{\beta}{3(\alpha\beta - \gamma^2)} \right| \\ &= \left| \frac{2m_2 m_3}{6e^{-2i\alpha_1} m_3 \cos^2 \theta_R + 3e^{-2i\alpha_2} m_3 \sin^2 \theta_R + 3e^{2i\alpha_1} m_2 \cos^2 \theta_R + 6e^{2i\alpha_2} m_2 \sin^2 \theta_R} \right. \\ &\quad \left. - \frac{1}{3} (m_3 \sin^2 \theta_R e^{-2i\alpha_2} + m_2 \cos^2 \theta_R e^{2i\alpha_1}) \right|,\end{aligned}\quad (57)$$

and for Model C

$$\begin{aligned}m_{ee} &= m_0^2 \left| (M_{R,C}^{-1})_{(1,1)} \right| = m_0^2 \left| \frac{2}{3\beta + 2\gamma} - \frac{\beta}{3(\alpha\beta - \gamma^2)} \right| \\ &= \left| \frac{2m_2 m_3}{3 [m_2 (\cos^2 \theta_R e^{i2\alpha_1} - \sin 2\theta_R e^{i(\alpha_1 + \alpha_2)}) + m_3 (\sin^2 \theta_R e^{-i2\alpha_2 + \sin 2\theta_R e^{-i(\alpha_1 + \alpha_2)}})]} \right. \\ &\quad \left. + \frac{1}{3} (m_2 \cos^2 \theta_R e^{2i\alpha_1} + m_3 \sin^2 \theta_R e^{-2i\alpha_2}) \right|.\end{aligned}\quad (58)$$

4.3 Numerical Result

In this section, we perform a numerical analysis for the parameters of Models B and C by applying the analytical expressions given in Eqs. (54)-(58). Though being expressed originally by five independent free parameters in the set $(|\alpha|, |\beta|, |\gamma|, \arg(\alpha), \arg(\beta))$, the predicted observables can also be expressed in terms of parameters $\alpha_1, \alpha_2, \theta_R, m_1, m_2, m_3$. These parameters can be further reduced by the using the values of $\sin^2 \theta_{13}, \Delta m_{12}^2$ and Δm_{23}^2 given by JUNO [5] and NuFIT [6] to compute θ_R, m_2 and m_3 . With Eqs. (55) or (56), m_1 can also be calculated using the correlations of their masses.

In total, fixing Eqs. (54)-(58) to the experimental observed values within a certain range of uncertainties can reduce the number of free parameters from 5 to 2 including the two phases α_1 and α_2 . Therefore, we can perform our numerical computations by freely sampling the two parameters α_1 and α_2 within the ranges $(0, 2\pi)$ to fit the remaining two observables, $\sin \theta_{12}$ and $\sin \theta_{23}$ within 1σ and 3σ .

The numerical results for the prediction of the effective neutrino mass parameter m_{ee} in neutrino-less double beta decay experimen with respect to the mass of lightest neutrino m_{lightest} are shown in Figure 3 for both Model B and Model C. These figures show the 1σ and 3σ ranges of oscillation parameters given by NuFiT 6.0 [6] (in blue) and JUNO (in red) for the normal ordering (NO) assuming $m_{\text{lightest}} = m_1$, and the inverted ordering (IO) assuming $m_{\text{lightest}} = m_3$. We also show the current upper limit of KamLAND-Zen experiment $(m_{ee})_{\text{upper}} = 0.028 - 0.122$ eV [45] and future sensitivities in JUNO-50T $(m_{ee})_{\text{upper}} = 0.005 - 0.012$ eV [46], in the figure. For correlation between mixing angels and δ , no distinguishable features except sum rules in Eq. (5) are predicted in Model A and Model B, and thus will not be shown.

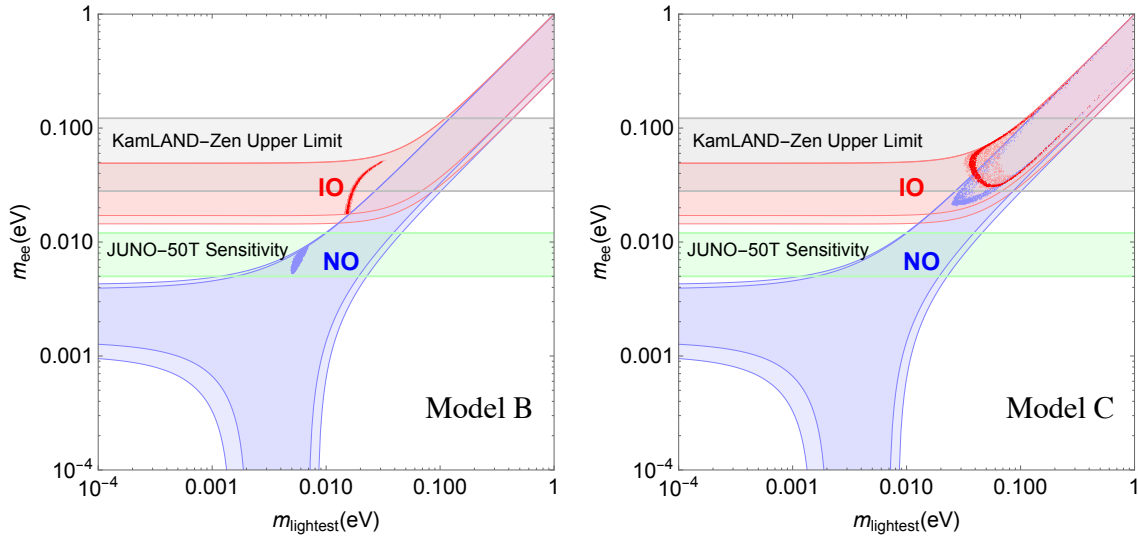


Figure 3: m_{lightest} vs m_{ee} predicted in Models B and C. Current experimental upper bound and future sensitivities on m_{ee} are shown as references.

5 Conclusions

This paper investigates the landscape of Models based on modular S_4 symmetry that predict the TM_1 pattern for neutrino mixing, and explores their parameter space compared with

the latest, high-precision neutrino oscillation data from the JUNO experiment. We first show the consistency of TM_1 mixing with JUNO data, and then gave a brief review on its realization by flavor symmetry. Starting from the permutation group S_4 , we showed that when the residual symmetry is assigned to be Z_3^T in the charged lepton sector and Z_2^{SU} in the neutrino sector, the model will predict the TM_1 mixing pattern. The result holds in both the traditional flavor models and modular flavor models.

We then explore three possible approaches for concrete model building in modular symmetries, as shown in Figure 1.

- In Model A, in the charged lepton sector, the breaking of $S_4 \rightarrow Z_3^T$ is ensured by the VEVs of a falvons aligned in a specific direction $\langle \varphi_\ell \rangle \sim (1, 0, 0)^T$, while in the neutrino sector, the breaking to Z_2^{SU} was due to the modular field τ_ν stabilizing at the fixed point $\langle \tau_\nu \rangle = \tau_{SU}$.
- In Model B, the residual symmetry Z_3^T in the lepton sector was realized by the modular field τ_ℓ stabilizing at the fixed point $\langle \tau_\ell \rangle = \tau_T$ giving rise to a diagonalized charged lepton mass matrix, while the residual symmetry Z_2^{SU} was enforced by the VEVs of two flavons aligned as $\langle \varphi_\nu \rangle \sim (1, 1, 1)^T$ and $\langle \varphi'_\nu \rangle \sim (0, 1, -1)^T$.
- In Model C, the modular symmetry acts on both the charged lepton and the neutrino sectors, thus a flavon Φ is needed to break the modular $S_4^\ell \times S_4^\nu$ symmetry to a diagonal S_4 subgroup. The two modular fields are then fixed at $\langle \tau_\ell \rangle = \tau_T$ and $\langle \tau_\nu \rangle = \tau_{SU}$ to realize the TM_1 mixing.

Each model have five free parameters to fit five observables, including two mass-squared differences and three mixing angles, while the Dirac CP phase is regarded as a prediction. For each model, we parameterize the explicit Majorana neutrino mass matrix by Eq. (49)-(48), which was then used to deduce analytical predictions and to do numerical fitting with datas from neutrino oscillation experiment.

Model A shows an over-restricted correlation between θ_{13} and neutrino masses and is thus excluded. However, it can be saved by arranging different modular weights to right-handed neutrinos with the price of more free parameters. We perform numerical scans for Models B and C using the analytical expressions derived in Eqs. (54)-(58). Parameter spaces consistent with the current bounds of neutrino oscillation parameters by JUNO and NuFIT was explored, and the predicted lightest neutrino masses m_{lightest} and m_{ee} was shown in Figure 3. Our results show that parameters in Model B and C best fit the latest result.

Acknowledgements:

This work is supported by National Natural Science Foundation of China (NSFC) under Grants Nos. 12205064, 12347103, and Zhejiang Provincial Natural Science Foundation of China under Grant No. LDQ24A050002.

References

- [1] S. Navas *et al.* [Particle Data Group], Phys. Rev. D **110** (2024) no.3, 030001 doi:10.1103/PhysRevD.110.030001
- [2] F. An *et al.* [JUNO], J. Phys. G **43** (2016) no.3, 030401 doi:10.1088/0954-3899/43/3/030401 [arXiv:1507.05613 [physics.ins-det]].
- [3] R. Acciarri *et al.* [DUNE], [arXiv:1512.06148 [physics.ins-det]].
- [4] K. Abe *et al.* [Hyper-Kamiokande], [arXiv:1805.04163 [physics.ins-det]].
- [5] A. Abusleme *et al.* [JUNO], [arXiv:2511.14593 [hep-ex]].
- [6] I. Esteban, M. C. Gonzalez-Garcia, M. Maltoni, I. Martinez-Soler, J. P. Pinheiro and T. Schwetz, JHEP **12** (2024), 216 doi:10.1007/JHEP12(2024)216 [arXiv:2410.05380 [hep-ph]]; NuFIT 6.0 (2024), www.nu-fit.org
- [7] G. J. Ding and J. W. F. Valle, Phys. Rept. **1109** (2025), 1-105 doi:10.1016/j.physrep.2024.12.005 [arXiv:2402.16963 [hep-ph]].
- [8] G. J. Ding and S. F. King, Rept. Prog. Phys. **87** (2024) no.8, 084201 doi:10.1088/1361-6633/ad52a3 [arXiv:2311.09282 [hep-ph]].
- [9] F. Feruglio and A. Romanino, Rev. Mod. Phys. **93** (2021) no.1, 015007 doi:10.1103/RevModPhys.93.015007 [arXiv:1912.06028 [hep-ph]].
- [10] Z. z. Xing, Phys. Rept. **854** (2020), 1-147 doi:10.1016/j.physrep.2020.02.001 [arXiv:1909.09610 [hep-ph]].
- [11] P. F. Harrison, D. H. Perkins and W. G. Scott, Phys. Lett. B **530** (2002), 167 doi:10.1016/S0370-2693(02)01336-9 [arXiv:hep-ph/0202074 [hep-ph]].
- [12] Z. z. Xing, Phys. Lett. B **533** (2002), 85-93 doi:10.1016/S0370-2693(02)01649-0 [arXiv:hep-ph/0204049 [hep-ph]].
- [13] F. P. An *et al.* [Daya Bay], Phys. Rev. Lett. **108** (2012), 171803 doi:10.1103/PhysRevLett.108.171803 [arXiv:1203.1669 [hep-ex]].
- [14] J. K. Ahn *et al.* [RENO], Phys. Rev. Lett. **108** (2012), 191802 doi:10.1103/PhysRevLett.108.191802 [arXiv:1204.0626 [hep-ex]].
- [15] C. H. Albright and W. Rodejohann, Eur. Phys. J. C **62** (2009), 599-608 doi:10.1140/epjc/s10052-009-1074-3 [arXiv:0812.0436 [hep-ph]].
- [16] C. H. Albright, A. Dueck and W. Rodejohann, Eur. Phys. J. C **70** (2010), 1099-1110 doi:10.1140/epjc/s10052-010-1492-2 [arXiv:1004.2798 [hep-ph]].
- [17] S. F. King and C. Luhn, Rept. Prog. Phys. **76**, 056201 (2013) doi:10.1088/0034-4885/76/5/056201 [arXiv:1301.1340 [hep-ph]].
- [18] W. Grimus and L. Lavoura, JHEP **09** (2008), 106 doi:10.1088/1126-6708/2008/09/106 [arXiv:0809.0226 [hep-ph]].

- [19] Z. z. Xing and S. Zhou, Phys. Lett. B **653** (2007), 278-287 doi:10.1016/j.physletb.2007.08.009 [arXiv:hep-ph/0607302 [hep-ph]].
- [20] X. G. He and A. Zee, Phys. Rev. D **84** (2011), 053004 doi:10.1103/PhysRevD.84.053004 [arXiv:1106.4359 [hep-ph]].
- [21] C. S. Lam, Phys. Rev. Lett. **101** (2008), 121602 doi:10.1103/PhysRevLett.101.121602 [arXiv:0804.2622 [hep-ph]].
- [22] I. de Medeiros Varzielas and L. Lavoura, J. Phys. G **40** (2013), 085002 doi:10.1088/0954-3899/40/8/085002 [arXiv:1212.3247 [hep-ph]].
- [23] C. Luhn, Nucl. Phys. B **875** (2013), 80-100 doi:10.1016/j.nuclphysb.2013.07.003 [arXiv:1306.2358 [hep-ph]].
- [24] F. Feruglio, doi:10.1142/9789813238053_0012 [arXiv:1706.08749 [hep-ph]].
- [25] J. T. Penedo and S. T. Petcov, Nucl. Phys. B **939** (2019), 292-307 doi:10.1016/j.nuclphysb.2018.12.016 [arXiv:1806.11040 [hep-ph]].
- [26] P. P. Novichkov, J. T. Penedo, S. T. Petcov and A. V. Titov, JHEP **04** (2019), 005 doi:10.1007/JHEP04(2019)005 [arXiv:1811.04933 [hep-ph]].
- [27] P. P. Novichkov, S. T. Petcov and M. Tanimoto, Phys. Lett. B **793** (2019), 247-258 doi:10.1016/j.physletb.2019.04.043 [arXiv:1812.11289 [hep-ph]].
- [28] T. Kobayashi, K. Tanaka and T. H. Tatsuishi, Phys. Rev. D **98** (2018) no.1, 016004 doi:10.1103/PhysRevD.98.016004 [arXiv:1803.10391 [hep-ph]].
- [29] I. de Medeiros Varzielas, S. F. King and Y. L. Zhou, Phys. Rev. D **101** (2020) no.5, 055033 doi:10.1103/PhysRevD.101.055033 [arXiv:1906.02208 [hep-ph]].
- [30] S. F. King and Y. L. Zhou, Phys. Rev. D **101** (2020) no.1, 015001 doi:10.1103/PhysRevD.101.015001 [arXiv:1908.02770 [hep-ph]].
- [31] S. Ge, C. Kong, and J. P. Pinheiro, [arXiv:2511.15422 [hep-ph]].
- [32] D. Zhang, [arXiv:2511.15654 [hep-ph]].
- [33] I. de Medeiros Varzielas and J. Lourenço, Nucl. Phys. B **979** (2022), 115793 doi:10.1016/j.nuclphysb.2022.115793 [arXiv:2107.04042 [hep-ph]].
- [34] H. Zhang and Y. L. Zhou, Int. J. Mod. Phys. A **39** (2024) no.05n06, 2450027 doi:10.1142/S0217751X24500271 [arXiv:2401.17810 [hep-ph]].
- [35] G. J. Ding, S. F. King, X. G. Liu and J. N. Lu, JHEP **12** (2019), 030 doi:10.1007/JHEP12(2019)030 [arXiv:1910.03460 [hep-ph]].
- [36] R. de Adelhart Toorop, F. Feruglio and C. Hagedorn, Nucl. Phys. B **858** (2012), 437-467 doi:10.1016/j.nuclphysb.2012.01.017 [arXiv:1112.1340 [hep-ph]].
- [37] I. de Medeiros Varzielas, M. Levy and Y. L. Zhou, JHEP **11** (2020), 085 doi:10.1007/JHEP11(2020)085 [arXiv:2008.05329 [hep-ph]].

- [38] S. F. King and Y. L. Zhou, JHEP **04** (2021), 291 doi:10.1007/JHEP04(2021)291 [arXiv:2103.02633 [hep-ph]].
- [39] C. Luhn, Nucl. Phys. B **875** (2013), 80-100 doi:10.1016/j.nuclphysb.2013.07.003 [arXiv:1306.2358 [hep-ph]].
- [40] S. F. King, Prog. Part. Nucl. Phys. **94** (2017), 217-256 doi:10.1016/j.ppnp.2017.01.003 [arXiv:1701.04413 [hep-ph]].
- [41] Y. Shimizu, M. Tanimoto and A. Watanabe, Prog. Theor. Phys. **126** (2011), 81-90 doi:10.1143/PTP.126.81 [arXiv:1105.2929 [hep-ph]].
- [42] S. F. King and C. Luhn, JHEP **09** (2011), 042 doi:10.1007/JHEP09(2011)042 [arXiv:1107.5332 [hep-ph]].
- [43] I. de Medeiros Varzielas and L. Lavoura, J. Phys. G **40** (2013), 085002 doi:10.1088/0954-3899/40/8/085002 [arXiv:1212.3247 [hep-ph]].
- [44] F. Bazzocchi, L. Merlo and S. Morisi, Nucl. Phys. B **816** (2009), 204-226 doi:10.1016/j.nuclphysb.2009.03.005 [arXiv:0901.2086 [hep-ph]].
- [45] S. Abe *et al.* [KamLAND-Zen], [arXiv:2406.11438 [hep-ex]].
- [46] J. Zhao, L. J. Wen, Y. F. Wang and J. Cao, Chin. Phys. C **41**, no.5, 053001 (2017) doi:10.1088/1674-1137/41/5/053001 [arXiv:1610.07143 [hep-ex]].